Bone 125 (2019) 140–150

Contents lists available at ScienceDirect

Bone

journal homepage: www.elsevier.com/locate/bone

Full Length Article

SDF-1/CXCR4 axis coordinates crosstalk between subchondral bone and articular cartilage in osteoarthritis pathogenesis

Han-Jun Qin[a,c,1], Ting Xu[d,1], Hang-Tian Wu[a,c], Zi-Long Yao[a,c], Yi-Long Hou[a,c], Yong-Heng Xie[a,c], Jian-Wen Su[a,c], Cai-Yu Cheng[a,c], Kai-Fan Yang[a,c], Xian-Rong Zhang[a,c], Yu Chai[a,b], Bin Yu[a,c,*], Zhuang Cui[a,c,*]

[a] Department of Orthopaedics and Traumatology, Nanfang Hospital, Southern Medical University, Guangzhou, Guangdong 510515, China
[b] Department of Orthopaedic Surgery, Institute for Cell Engineering, Johns Hopkins University, Baltimore, MD 21205, USA
[c] Key Laboratory of Bone and Cartilage Regeneration Medicine, Southern Medical University, Guangzhou, Guangdong 510515, China
[d] Department of Sleep Medicine Center, Nanfang Hospital, Southern Medical University, Guangzhou, Guangdong 510515, China

ARTICLE INFO

Keywords:
Osteoarthritis
Subchondral bone
SDF-1
CXCR4
Cartilage

ABSTRACT

Crosstalk between subchondral bone and articular cartilage is considered a central feature of osteoarthritis (OA) initiation and progression, but its underlying molecular mechanism remains elusive. Meanwhile, specific administration of drugs in subchondral bone is also a great challenge during investigation of the process. We here explore the role of stromal cell-derived factor 1 (SDF-1)/C-X-C chemokine receptor type 4 (CXCR4) axis in the crosstalk between subchondral bone and articular cartilage in OA pathogenesis, using osmotic infusion pumps implanted in tibial subchondral bone directly to ensure quantitative, continuous and steady drug delivery over the entire experiment. We found that increased SDF-1 in subchondral bone firstly induced subchondral bone deterioration by erroneous Mesenchymal Stem Cells (MSCs) recruitment and excessive bone resorption in anterior cruciate ligament transection (ACLT) mice. Deterioration of subchondral bone then led to the traverse of SDF-1 from subchondral bone to overlying cartilage. Finally, SDF-1 from underlying subchondral bone combined with CXCR4 in chondrocytes to induce articular cartilage degradation by promoting the shift of transforming growth factor-β receptor type I (TβRI) in chondrocytes from activin receptor-like kinase 5 (ALK5) to activin receptor-like kinase 1 (ALK1). More importantly, specific inhibition of SDF-1/CXCR4 axis in ACLT rats attenuated OA by stabilizing subchondral bone microarchitecture, reducing SDF-1 in cartilage and abrogating the shift of TβRI in chondrocytes. Our data demonstrate that the SDF-1/CXCR4 axis may coordinate the crosstalk between subchondral bone and articular cartilage in OA pathogenesis. Therefore, specific inhibition of SDF-1/CXCR4 axis in subchondral bone or intervention in SDF-1 traverse may be therapeutic targets for OA.

1. Introduction

Osteoarthritis (OA) is the most common multifactorial degenerative joint disorders characterized by cartilage loss, subchondral bone sclerosis and osteophyte formation [1–3]. Current pharmacologic therapies primarily target at symptoms controlling but their efficacy on OA progression is disappointing, until the end stage necessitating joint replacement [4,5]. As the exact pathogenesis of OA remains elusive, explorations for targets in preventive and disease-modifying therapies are urgently needed.

It is now recognized that although OA is characterized by articular cartilage degeneration the whole joint is involved during OA progression [6–9]. Notably, the crosstalk between subchondral bone and articular cartilage is also considered a central feature of OA initiation and progression [10–12]. It has been reported that the alteration in subchondral bone microarchitecture precedes articular cartilage degeneration during OA progression [13–16]. We have also found that uncoupled bone remodeling plays a pivotal role in the cartilage degeneration [17,18]. Of note, cartilage chondrocytes in OA are different from normal cartilage ones in their cytokine and growth factor expression patterns [19,20]. Previous studies have reported that both OA and the aging process itself alter the pattern of TβRI expression in a

* Corresponding authors at: Department of Orthopaedics and Traumatology, Nanfang Hospital, Southern Medical University, Guangzhou, Guangdong 510515, China.
E-mail addresses: cuizhuang@smu.edu.cn (B. Yu), yubinol@163.com (Z. Cui).
[1] Han-Jun Qin and Ting Xu have contributed equally to this work.

https://doi.org/10.1016/j.bone.2019.05.010
Received 20 December 2018; Received in revised form 20 April 2019; Accepted 7 May 2019
Available online 17 May 2019

shift from ALK5 to ALK1 [21]. The impact of TGF-β on cartilage is anabolic through ALK5 induced Smad2/3 signaling [22] while catabolic through ALK1 induced Smad1/5/8 signaling pathway [23–25]. However, the underlying mechanism remains unknown towards the shifting of receptor balance between ALK1 and ALK5 in chondrocytes during OA pathogenesis.

Consideration of the crosstalk between subchondral bone and overlying cartilage as a main factor in OA initiation and progression raises a question. Is it feasible that the mutual communication occurs between subchondral bone and articular cartilage? It is known that the interface between the subchondral bone and calcified layer of cartilage lies subchondral bone plate (SBP), which acts as an impenetrable barriers to sustain the homeostasis and integrity of overlying cartilage [26,27]. However, increasing evidence shows that it is probable for them to communicate. Several studies have demonstrated that the subchondral plate porosity increases in OA [28,29], accompanied by accumulation of microcracks and eruption of blood vessels through the plate, implying that molecules may traverse the subchondral plate to couple subchondral bone deterioration and articular cartilage degeneration during OA progression.

Stromal cell-derived factor 1 (SDF-1), an 8-kDa chemokine, exerts its role by binding to the seven transmembrane G-protein-coupled receptor, C-X-C chemokine receptor type 4 (CXCR4). It is reported that SDF-1 is mainly expressed by bone marrow stromal stem cells [30] and osteoblasts [31] in bone but not produced by chondrocytes in cartilage [32,33]. Recent evidence has attracted more attention towards the role of SDF-1/CXCR4 axis in the OA pathogenesis. Previous studies have showed that SDF-1 increases dramatically in the synovial fluid [34,35] and subchondral bone [36] while the expression of its receptor CXCR4 elevates significantly in the articular chondrocytes and subchondral bone marrow stromal cells [36,37]. These imply that SDF-1/CXCR4 axis may play a vital role in OA progression, but it is unknown whether and how SDF-1/CXCR4 axis regulates the crosstalk between subchondral bone and articular cartilage in OA pathogenesis.

Thus in the present study, we inserted and fixed osmotic infusion pumps directly in subchondral bone as a local drug delivery tool which allows quantitative, continuous and steady drug delivery over the entire experiment. Our results revealed that SDF-1/CXCR4 axis might coordinate the crosstalk between subchondral bone and articular cartilage in OA pathogenesis and that specific inhibition of SDF-1/CXCR4 axis attenuated OA by stabilizing subchondral bone microarchitecture, reducing SDF-1 in cartilage and abrogating the shift of TβRI in chondrocytes.

2. Materials and methods

2.1. Mice, rats and clinical samples

Three-month-old male C57BL/6J (WT) mice and SD rats were purchased from the animal center of Southern Medical University. The anterior cruciate ligament transection (ACLT) was done to induce abnormal mechanical loading-associated osteoarthritis of the left knee. Sham operation was done by opening the joint capsule and then suturing the incision in the left knee of independent rodents. Mice were used for the study of the effect of systemic drug administration on OA development. We randomly divided the mice into 3 groups as follows: sham-operated, ACLT-operated treated with vehicle and ACLT-operated treated with AMD3100 (n = 15 per group, 5 on day 14, 30 and 60 separately). Rats were introduced to explore the effect of local administration of drug in subchondral bone on OA development. Rats were also randomized to similar 3 groups (n = 5 per group). Rats were euthanized 2 months after surgery. All mice and rats were maintained in the Animal Facility of the Southern Medical University. The experimental protocols were reviewed and approved by the Institutional Animal Care and Use Committee of the Southern Medical University, Guangzhou, China. Additionally, Various regions of human OA joints were harvested from the human subjects undergoing total knee replacement (n = 4, age range 50-70 years old). The integrated samples were divided into OA part and relatively normal part (RN). OA group where cartilage was severely damaged or fibrillated with OARSI score of 15–18; while relatively normal (RN) group was non-fibrillated with OARSI scores of 0–3 [36]. ALL personal information was anonymized and de-identified and this study was approved by the Ethical Medical Committee, Nanfang Hospital.

2.2. Implantation of osmotic infusion pumps

Both systemic and local administration of AMD3100 were administrated directly after ACLT surgery. For systemic admission of AMD3100 (Abcam, ab120718) in ACLT mice, a 1.5 cm transverse skin incision was made over the dorsal thorax, and a subcutaneous pocket created via blunt dissection. The loaded Alzet osmotic minipumps (Alzet model 1004, 0.11 μl per hour, 28 days) were inserted and the fascia and skin closed with 8–0 nylon. AMD3100 was delivered at a rate of 180 μg/day, which corresponds to steady serum level of 0.3 μg/ml [38–40,49].

For specific administration of AMD3100 in tibial subchondral bone of ACLT rats, a curved incision was made on the lateral side of the knee. The incision began from the level of the knee and ended to 1 cm distal to the tibial tuberosity. We then made a layer-by-layer dissection to expose tibial anterolateral muscles and bluntly dissected them along the lateral border of the tibia. To avoid blockage of micro-osmotic pumps, we first inserted a 1 ml syringe needle from the anteroinferior tibial plateau and confirmed the needle in subchondral bone by X-ray. Then, micro-osmotic pumps (Alzet model 1004, 0.11 μl per hour, 28 days) were implanted into subchondral bone following the canal made by the syringe needle and covered by anterolateral muscles. Finally, the whole assembly was buried subcutaneously. AMD3100 (1 μg) was infused into subchondral bone continuously for 1 month employing osmotic infusion pump.

2.3. Micro-CT analysis

We acquired the knee joints of mice and rats and dissected them free of soft tissue, fixed them in 70% ethanol overnight. We then scanned the specimen using high-resolution micro-CT (SkyScan 1172) and reconstructed the scanned images by image reconstruction software (NRecon v1.6) [16]. The data were analyzed using data analysis software (CTAn v1.9) and three-dimensional model visualization software (μ CTVol v2.0). We set the scanner at a voltage of 50 kVp, current of 200 μA and resolution of 5.8 μm per pixel. We chose a threshold of 50 based on visual interpretation. Three-dimensional histomorphometric analysis was performed using longitudinal images of the tibial subchondral bone. The region of interest was defined to cover the whole tibial subchondral bone medial compartment. Three-dimensional structural parameters analyzed included: TV (total tissue volume; contains both trabecular and cortical bone), Tb.Th (trabecular thickness), Tb.Sp (trabecular separation), Conn.Dn (connectivity density) and Tb.Pf (trabecular pattern factor).

2.4. Fluorescence in Situ Hybridization for SDF-1

Slides were placed in a wet box and applied with 0.2 mol/L hydrochloric acid to the tissue. We rinsed the slices for 15 min at room temperature and washed them twice with DEPC for 1 min each time. The slices were covered with Proteinase K and put into the molecular hybridizer at 37 °C for 20 min. Proteinase K reaction was stopped with 0.2% or 0.1 mol/L glycine wash solution for 1 min (fresh) followed by wash twice in PBS, 1 min each time. We fixed tissue with 4% PFA paraformaldehyde for 10 min, then washed three times in PBS for 1 min each time. The slices were washed twice with acetic anhydride (pH = 8.0) at room temperature for 5 min followed by wash 5 times

with PBS for 1 min each time, then washed twice with 5 × SSC (pH 7.5) for 1 min each. The slices were put in wet box and FISH probes (Mus SDF-1 5′-FAM-CCGGCAGGGGCAUCGGUAGCUCAGGCUGAC-3′) were applied to the slides, and hybridized at 37 °C overnight. Then the slices were washed with 2 × SSC (pH = 7.5) at room temperature for 1 min followed by wash 5 times with PBS for 1 min each at room temperature.

2.5. Histochemistry, immunohistochemistry and histomorphometry analysis

Knee joints of mice and rats were dissected, fixed in 4% buffered formalin for 48 h, and decalcified in 10% EDTA (pH 7.4) for 4 weeks. Specimens were embedded in either paraffin or optimal cutting temperature (OCT) compound (Sakura Finetek). 4-μm-Thick longitudinal-oriented sections of the knee joint medial compartment were cut. For the measurement of the thickness of the calcified cartilage in H&E staining, 10× modified images were selected. Hyaline cartilage was separated from calcified cartilage by the tidemark line. We measured the distance from the tidemark to subchondral bone plate (SBP) as the thickness of calcified cartilage, and the distance from the tidemark to articular cartilage surface as the thickness of hyaline cartilage. Tartrate-resistant acid phosphatase (Trap) staining was conducted using a standard protocol (Sigma-Aldrich). Sagittal sections of knee joint medial compartment were incubated with primary antibodies at 4 °C overnight. For immunohistochemical staining, we used a horseradish peroxidase-streptavidin detection system (Dako) and counterstained with hematoxylin (Dako) or methyl green (Sigma-Aldrich). For immunofluorescence staining, second antibodies conjugated with fluorescence were incubated for 1 h at room temperature (RT) while avoiding light. We then microphotographed slices to perform histomorphometric measurements on the entire area of the tibia subchondral bone (Olympus DP71). Quantitative analysis was conducted in a blinded fashion with software image J (ImageJ 1.51j8). The number of positively stained cells was counted in the whole tibia subchondral bone area per specimen and five sequential specimens per mouse in each group were measured. Osteoarthritis Research Society International-modified Mankin criteria (OARSI) scores were calculated as previously described [41].

2.6. Chondrocytes and BMCs culture

Chondrocytes were isolated from the epiphyses of long bones of the hind limb from 3 to 4 day old C57BL/6J mice. Surrounding tissues were dissected clearly by two tweezers and epiphyseal cartilage were collected in DMEM/F12 medium. The tissue was exposed to 0.25% trypsin 0.9 mM EDTA for 15 min, and subsequently incubated with 0.15% collagenase type II for 3–4 h at 37 °C with continuous mixing. Digested cartilage was strained through a 70 μm membrane and cells collected by centrifugation and cultured in DMEM/F12 medium supplemented with 10% fetal bovine serum at 37 °C in a humidified 5% CO2 incubator. Four week-old C57BL/6J mice were sacrificed and the primary BMSCs were isolated from the femurs and tibias under a sterile condition. After flushing the bone marrow cavity with MEM alpha medium and removing large tissues with a 200-mesh nylon filter, the isolated bone marrow cells were cultured in MEM alpha medium supplemented with 10% fetal bovine serum, 1% penicillin and streptomycin at 37 °C in an environment with 5% CO2.

2.7. Transwell assay

The migration assay was designed using transwell plates that were 6.5 mm in diameter with 8 μm pore filters. The upper chambers were loaded with 1×10^5 BMSCs in 200 μl of DMEM containing 0.1% BSA, and the lower chambers with 500 μl of DMEM containing 10% FBS. In SDF group the lower chambers were treated with SDF-1 (100 ng/ml). In AMD group, the BMSCs in upper chambers were 2 hr-pretreatment of 200 ng/ml AMD3100, the lower chambers were treated with SDF-1 (100 ng/ml). Following incubation for 15 h, cells in the upper chamber were removed and the membranes were fixed in 4% paraformaldehyde for 20 min. The cells that migrated to the lower side of the filter were stained with 0.1% crystal violet for 10 min and then observed under a light microscope [42].

2.8. Mechanical stress trial

To investigate the effect of tensile forces itself on the pattern of TβRI expression in chondrocytes, we conducted the mechanical stress trial in vitro. Chondrocytes (5 × 105/well), cultured in DMEM/F12 medium supplemented with 10% FBS and 100 μg/ml streptomycin and 100 U/ml penicillin, were grown on collagen type I-coated Bioflex II, six-well culture plates to 80% confluence (7–8 days). Various magnitudes (0, 3%, 6%, 9%, 12%, 18%) of Cyclic Tensile Stress (CTS) were applied to the cells at a rate of 0.5 Hz by FX-5000 Flexercell system (Flexcell International) [43]. After loading of the plates on a station (located in an incubator at 5% CO2 with 95% humidity) for 24 h, protein was extracted for Western Blot analysis.

2.9. RT-PCR

To determine the effect of SDF-1 on the gene expression of ALK1 and ALK5 in chondrocytes, primary mouse articular chondrocytes were treated with 0, 20, 50 ng/ml SDF-1 for 24 h with or without 2 hr-pretreatment of 200 ng/ml AMD3100. Before the treatment of SDF-1, the culture medium of chondrocytes was changed into DMEM/F12 medium supplemented with 1% FBS. The TRIzol reagent (Invitrogen, CA, United States) was used for homogenization and the total RNA extraction was conducted following the manufacturer's instructions. PrimeScript™ RT Master Mix (Takara) was employed to reverse transcribe mRNA into cDNA and SYBR® Premix Ex Taq™ II PCR was used to perform RT-PCR on ABI QuantStudio5 (Applied Biosystems USA). The relative expression of each target gene (ALK1 and ALK5) was calculated using the $2^{-\Delta\Delta Ct}$ method. The primer sequences for the genes used are listed in Supplementary Table 1.

2.10. Western blot

To detect the effect of SDF-1 on the relative protein expression in chondrocytes, primary mouse articular chondrocytes were plated on 6-well plates and treated with 0, 20, 50 ng/ml SDF-1 for 24 h with or without 2 hr-pretreatment of 200 ng/ml AMD3100. Before the treatment of SDF-1, the culture medium of chondrocytes was changed into DMEM/F12 medium supplemented with 1% FBS. Extracted protein (30 μg) were separated using SDS-PAGE and blotted on polyvinylidene fluoride (PVDF) membrane (Bio-Rad Laboratories). Proteins were analyzed for ALK1 (Thermo Fisher, 1:1000, PA5-49803), ALK5 (Abcam, 1:500, ab31013) and CXCR4 (Abcam, 1:100, ab124824) and visualized by an enhanced chemiluminescence kit (Amersham Bioscience).

2.11. Statistical analysis

Experiments were performed three times. Data are presented as mean ± s.d. One-way analysis of variance (ANOVA) was used for multifactorial comparisons in this study. Homogeneity of variance was tested first and then the differences between groups were assessed by post hoc multiple comparisons. Specifically, if no heterogeneity was observed, the Bonferroni test was used to assess the differences between groups. However, if heterogeneity did exist, the Welch test was used to test the equality of means and the Dunnett's T3 was used to assess the differences between groups. The investigators were blinded to allocation during experiments and outcome assessment. The level of significance was set at $P < 0.05$ and indicated by "*" compared as denoted by bar, $P < 0.01$ was indicated by "**" compared as denoted by bar. All data analysis was conducted with SPSS 22.0 analysis software

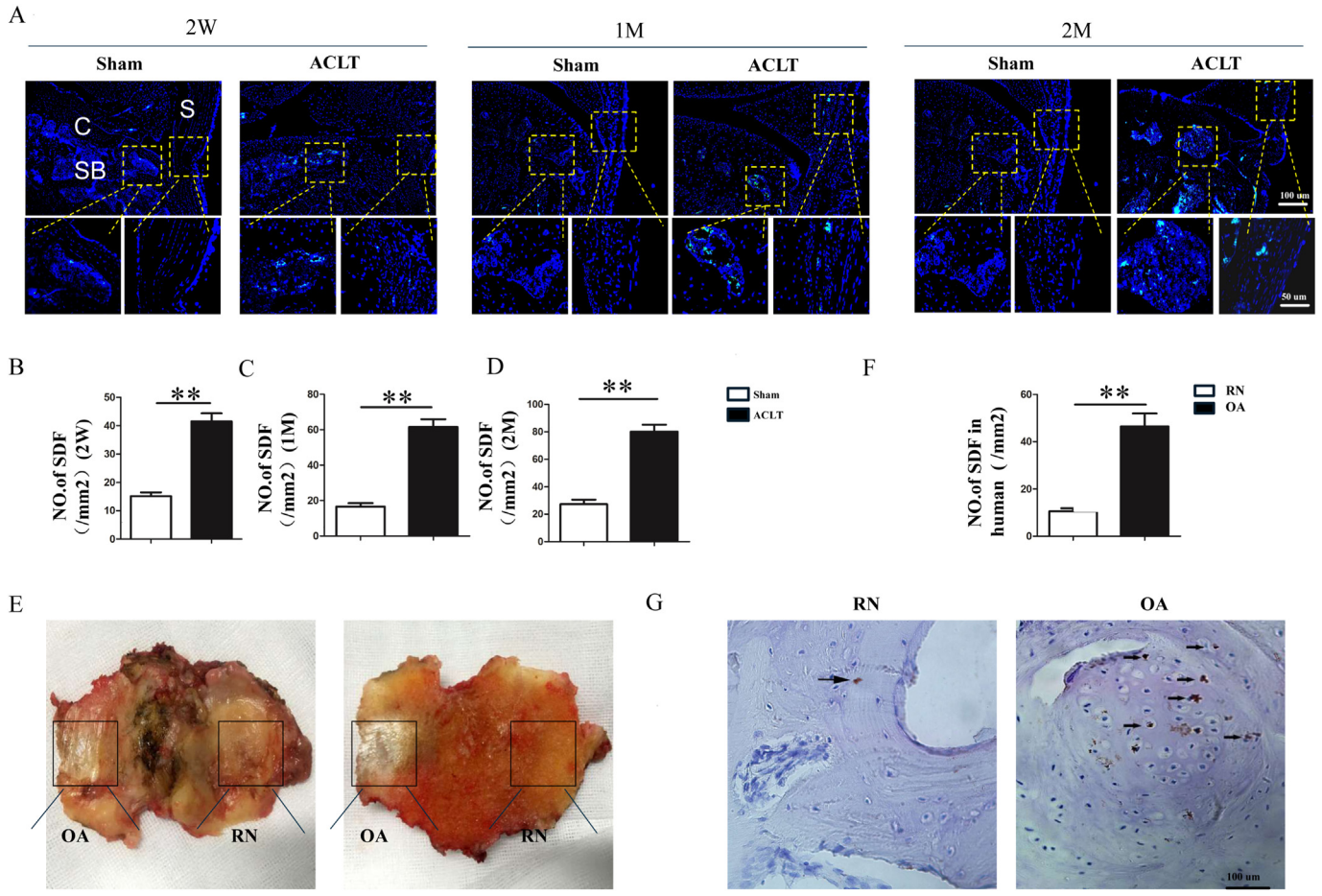

Fig. 1. SDF-1 elevates in subchondral bone during the onset of OA. (A–C) Immunofluorescent staining and quantitative analysis of SDF-1 in subchondral bone of ACLT mice at 14, 30 and 60 days post operation. $n = 5$. Scale bar, 100 μm; Magnified view, 50 μm. SB = Subchondral bone; C = Cartilage; S = Synovium. (D) The gross macroscopic observation in tibial plateau of the samples obtained from patients at the time of total joint arthroplasty. OA = Osteoarthritis damaged part; RN = relatively normal part. (E, F) Immunohistochemical staining of SDF-1 in human subchondral bone of OA part and RN part. $N = 4$. Scale bar, 100 μm. Sham = sham-surgery. ACLT = ACLT-surgery treated with vehicle. $^{*}p < 0.05$, $^{**}p < 0.01$ compared as denoted by bar.

(SPSS Inc.).

3. Results

3.1. SDF-1 elevates in subchondral bone during the onset of OA

Recent evidence has attracted more attention towards the role of SDF-1/CXCR4 axis in the OA pathogenesis. Immunofluorescent staining showed that the level of SDF-1 elevated significantly in the subchondral bone of ACLT mice in comparison with sham controls (Fig. 1A–C). Consistently, a higher level of SDF-1 was detected in the OA part of human subchondral bone compared to the RN part (Fig. 1D–F and Supplementary Fig. 1). We next examined the effects of inhibition of SDF-1/CXCR4 axis on the joints in ACLT mice by systemic administration of AMD3100. Three-dimensional micro-CT of tibial subchondral bone showed increased TV and Tb.Pf, and reduced SBP thickness in ACLT mice since 14 d after surgery. However, treatment with AMD3100 returned these parameters back to their normal levels comparable with sham controls (Fig. 2A–D and Supplementary Fig. 2). In addition, we found that articular cartilage degeneration began 30 d after surgery, following subchondral bone deterioration (Fig. 2A and E). Inhibition of SDF-1/CXCR4 axis normalized OARSI scores and the expression levels of MMP13, Col X and ADAMTS5 in articular cartilage similar to sham controls (Fig. 2F–J). These findings demonstrated that inhibition of SDF-1/CXCR4 axis ameliorated OA pathogenesis by normalization of subchondral bone deterioration and further rescue of the homeostasis and integrity of overlying cartilage.

3.2. SDF-1/CXCR4 axis induces subchondral bone deterioration by erroneous recruitment of MSCs and excessive bone resorption

We then explore the mechanism of SDF-1/CXCR4 axis on the alteration of subchondral bone microarchitecture in ACLT mice in OA pathogenesis. We found that the MSCs were increased significantly and dispersed throughout the bone marrow in subchondral bone of vehicle-treated ACLT mice and that inhibition of SDF-1/CXCR4 axis returned the MSCs back to normal comparable with sham controls (Fig. 3A and D). We further confirmed that SDF-1/CXCR4 axis induced the mobilization and recruitment of MSCs as demonstrated by the transwell assay (Fig. 3K and L). And the amount of $pErK^{+}$ and $osterix^{+}$ cells [44,45] were dramatically higher in subchondral bone of vehicle-treated ACLT mice in comparison with AMD3100-treated ACLT group (Fig. 3E–H). In addition, the number of tartrate-resistant acid phosphatase (TRAP)-positive osteoclast cells increased dramatically (Fig. 3I–J) and led to larger bone marrow cavities (Fig. 2A–D) in the vehicle-treated ACLT model in comparison with sham controls. Of note, inhibition of SDF-1/CXCR4 axis suspended the elevation of $TRAP^{+}$ cells and normalized subchondral bone microarchitecture. Taken together, these results suggested that, during OA pathogenesis, SDF-1/CXCR4 axis might induce subchondral bone deterioration by erroneous recruitment of MSCs and excessive bone resorption.

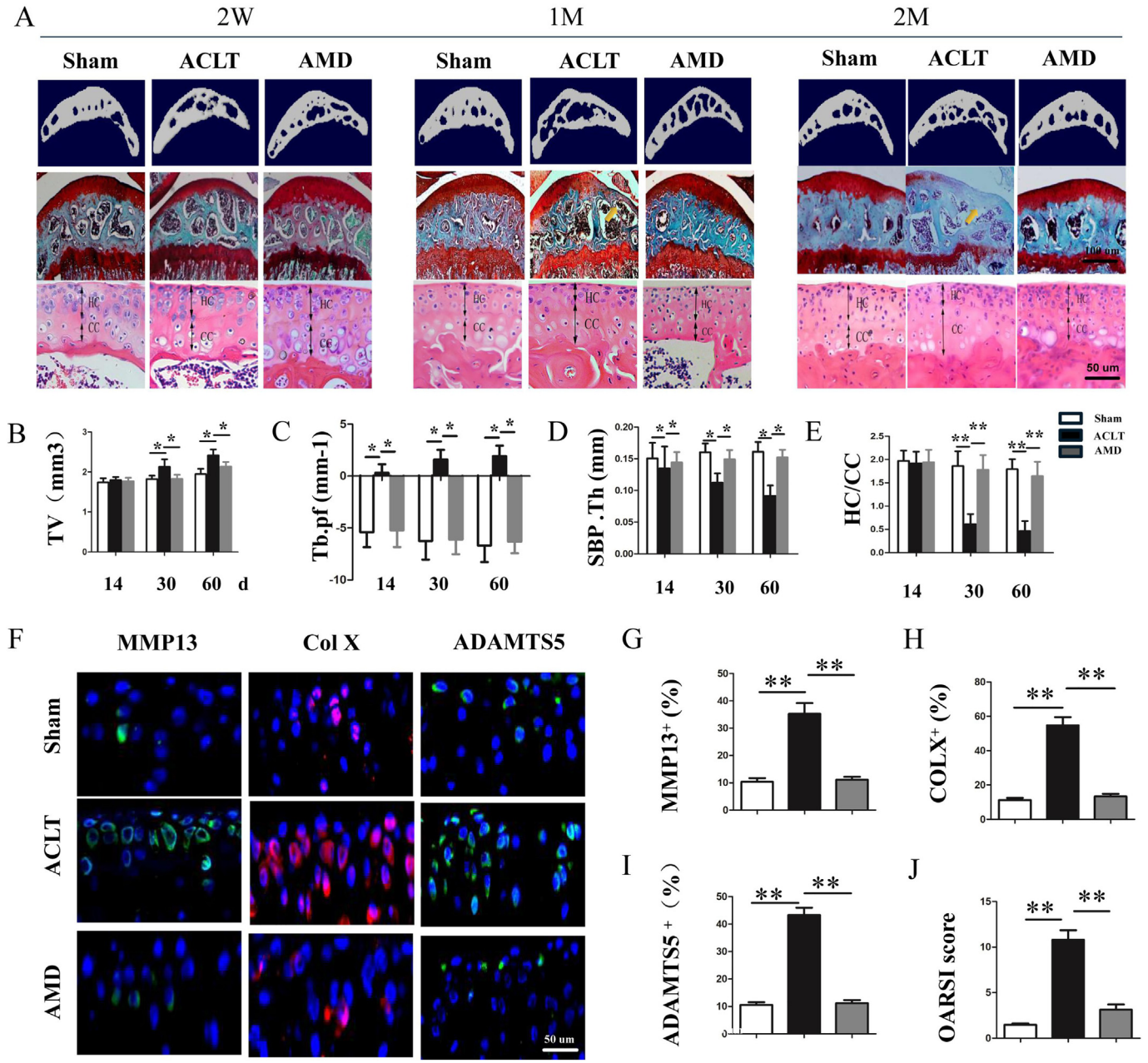

Fig. 2. Inhibition of SDF-1/CXCR4 axis systemically attenuates OA pathogenesis in mice. (A) Representative three dimensional micro-CT images of sagittal views of subchondral bone medial compartment (TOP); Safranin O and fast green staining (middle) with solid arrows indicating proteoglycan loss and cartilage destruction (Scale bar, 100 μm); H&E staining (bottom) where double-headed arrows to marker calcified cartilage (CC) and hyaline cartilage (HC) thickness (Scale bars, 50 μm) at 14, 30 and 60 days after sham operation or ACLT surgery. (B–E) Quantitative analysis of tibial subchondral bone of total tissue volume (TV) (B), trabecular pattern factor (Tb.pf) (C), subchondral bone plate thickness (D) and HC/CC ratio in cartilage (E) $n = 5$ per group. (F–I) Immunostaining and quantification of MMP13, Col X and ADAMTS5 in articular cartilage 30 d post-operation. n = 5 per group. Scale bars, 50 μm. (J) Osteoarthritis Research Society International-modified Mankin scores of articular cartilage at 30 days after surgery. $n = 5$. Sham = sham-surgery; ACLT = ACLT-surgery treated with vehicle; AMD = ACLT-surgery treated with AMD3100. $^{*}p < 0.05$, $^{**}p < 0.01$ compared as denoted by bar.

3.3. SDF-1 in cartilage elevates following subchondral bone deterioration

Double-immunofluorescent staining showed that the amount of SDF-1 in articular cartilage elevated significantly in vehicle-treated ACLT mice in comparison with sham controls, while inhibition of SDF-1/CXCR4 axis normalized the SDF-1 level in cartilage (Fig. 4A and B). Moreover, we further found that specific administration of AMD3100 in subchondral bone returned the elevated SDF-1 in articular cartilage back to normal level in comparison with vehicle-treated ACLT rats (Fig. 4C and D). However, mRNA expression of SDF-1 was not detected in chondrocytes though it is obvious in the cells of subchondral bone in ACLT mice, demonstrated by in-situ hybridization (Supplementary Fig. 3). In addition, we found expression of CXCR4 in cartilage was increased in vehicle-treated ACLT mice during OA pathogenesis whereas inhibition of SDF-1/CXCR4 axis returned the elevated CXCR4 back to normal level (Fig. 4E and F), which was confirmed by the western-blot assay (Fig. 4G). These results indicated that SDF-1 in subchondral bone might traverse from bone to cartilage to link subchondral bone deterioration with articular cartilage degeneration.

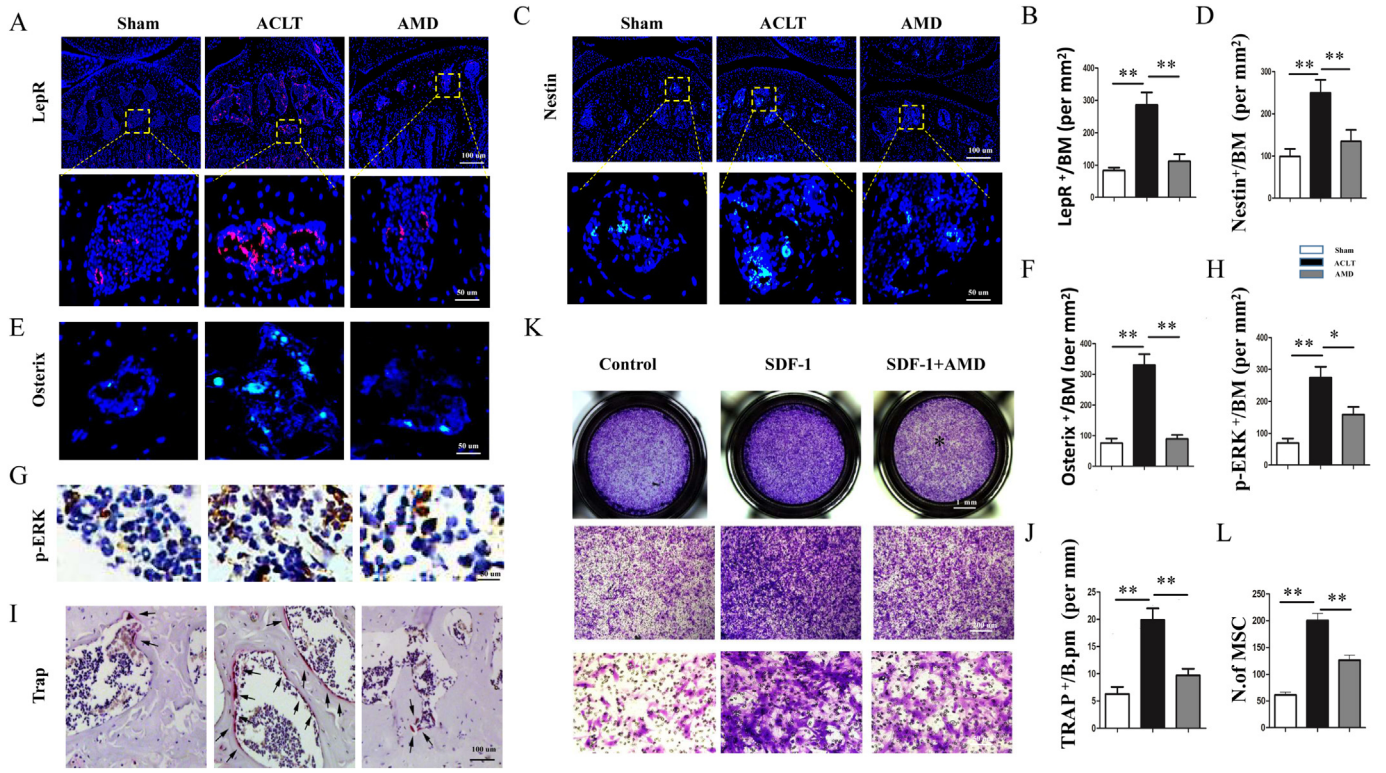

Fig. 3. SDF-1/CXCR4 axis induces subchondral bone deterioration by erroneous recruitment of MSCs and excessive bone resorption in mice. (A–H) Immunostaining and quantitative analysis of LepR+ (A,B), nestin$^+$ (C, D), osterix$^+$ (G, H) and pErk$^+$ (E, F) cells in subchondral bone at 30 days post operation. $n = 5$ per group. Scale bar, 100 μm; Magnified view, 50 μm. (I, J) Tartrate-resistant acid phosphatase (TRAP) staining and quantitative analysis from mice at 30 days after surgery. $n = 5$. Scale bar, 100 μm. (K, L) Transwell assay. Immunostaining and quantification of MSCs induced by SDF-1. Sham = sham-surgery; ACLT = ACLT-surgery treated with vehicle; AMD = ACLT-surgery treated with AMD3100. $*p < 0.05$, $**p < 0.01$ compared as denoted by bar.

3.4. SDF-1/CXCR4 axis induces articular cartilage degradation by promoting shift of TβRI expression in chondrocytes from ALK5 to ALK1

It has been reported that the ALK1/ALK5 ratio increases during OA progression [25], but the underlying mechanism is still unknown. The present study confirmed that the reduction of ALK5 was much greater during the onset of OA than that of ALK1 in ACLT mice (Fig. 5A–D), resulting in the elevated ratio of ALK1/ALK5. We also found that the ALK1/ALK5 ratio was regulated by SDF-1/CXCR4 axis and that inhibition of SDF-1/CXCR4 axis with AMD3100 increased the expression of ALK5 but reduced the ALK1 level in articular cartilage (Fig. 5A–D). Consistently, our western-blot analysis (Fig. 5E) and RT-PCR (Fig. 5F and G) showed that SDF-1 reduced ALK5 expression but kept ALK1 expression in chondrocytes while inhibition of SDF-1/CXCR4 axis increased the expression of ALK5 but decreased ALK1 level. We further confirmed that the abnormal mechanical stress itself on chondrocytes did not alter the ALK5 and ALK1 expression (Fig. 5H). Taken together, these results revealed that SDF-1/CXCR4 axis induced articular cartilage degeneration by promoting the shift of TβRI in chondrocytes from ALK5 to ALK1 during OA pathogenesis.

3.5. Specific inhibition of SDF-1/CXCR4 axis in subchondral bone using osmotic infusion pumps attenuates OA

To validate the role of SDF-1/CXCR4 axis in subchondral bone during the onset of OA, specific inhibition of SDF-1/CXCR4 axis in the subchondral bone of ACLT rats was achieved via osmotic infusion pumps (Fig. 6A and B). Like systemic use of SDF-1/CXCR4 axis inhibitor, local application of AMD3100 similarly improved the subchondral bone microarchitecture in comparison with vehicle-treated ACLT rats (Fig. 6C–G and Supplementary Fig. 2). Further specific inhibition of SDF-1/CXCR4 axis suspended the elevation of nestin$^+$ and MMP9$^+$ cells in subchondral bone as compared to vehicle-treated ACLT controls (Fig. 6H–K). In addition, we found that specific inhibition of SDF-1/CXCR4 axis in subchondral bone attenuated articular cartilage degeneration, as demonstrated in OARSI scores (Fig. 6C and L). Moreover, specific inhibition of SDF-1/CXCR4 axis normalized the expression of MMP13, Col X and ADAMTS5 in articular cartilage as in sham controls (Fig. 6M–P). In exploration of the chondroprotective mechanism for specific inhibition of SDF-1/CXCR4 axis using osmotic infusion pumps in subchondral bone, we found that specific administration of AMD3100 in the subchondral bone returned the SDF-1 in the articular cartilage back to its normal level in comparison with vehicle-treated ACLT controls (Fig. 4C and D). More importantly, as in sham controls, specific inhibition of SDF-1/CXCR4 axis in the subchondral bone normalized the ALK1/ALK5 ratio in articular cartilage which was increased significantly in the vehicle-treated ACLT rats (Fig. 6Q–T). Taken together, all these results demonstrated that SDF-1/CXCR4 axis exerted its role on OA pathogenesis as a coupling factor between subchondral bone and articular cartilage.

4. Discussion

Subchondral bone deterioration plays a central role in triggering a cascade of events that lead to overlying cartilage degeneration, then the onset of OA [9,16]. In this study, we demonstrated that SDF-1/CXCR4 axis coordinated the crosstalk between subchondral bone and articular cartilage in OA pathogenesis. Specific inhibition of SDF-1/CXCR4 axis attenuated OA by stabilizing subchondral bone microarchitecture, reducing SDF-1 in cartilage and abrogating the shift of TβRI in chondrocytes. We also noticed that SDF-1 in synovium has been reported to play a vital role in cartilage degeneration by infiltrating into chondrocytes [35], and that synovectomy could ameliorate the onset of OA [34]. We believe in these findings as we consider that SDF-1 in

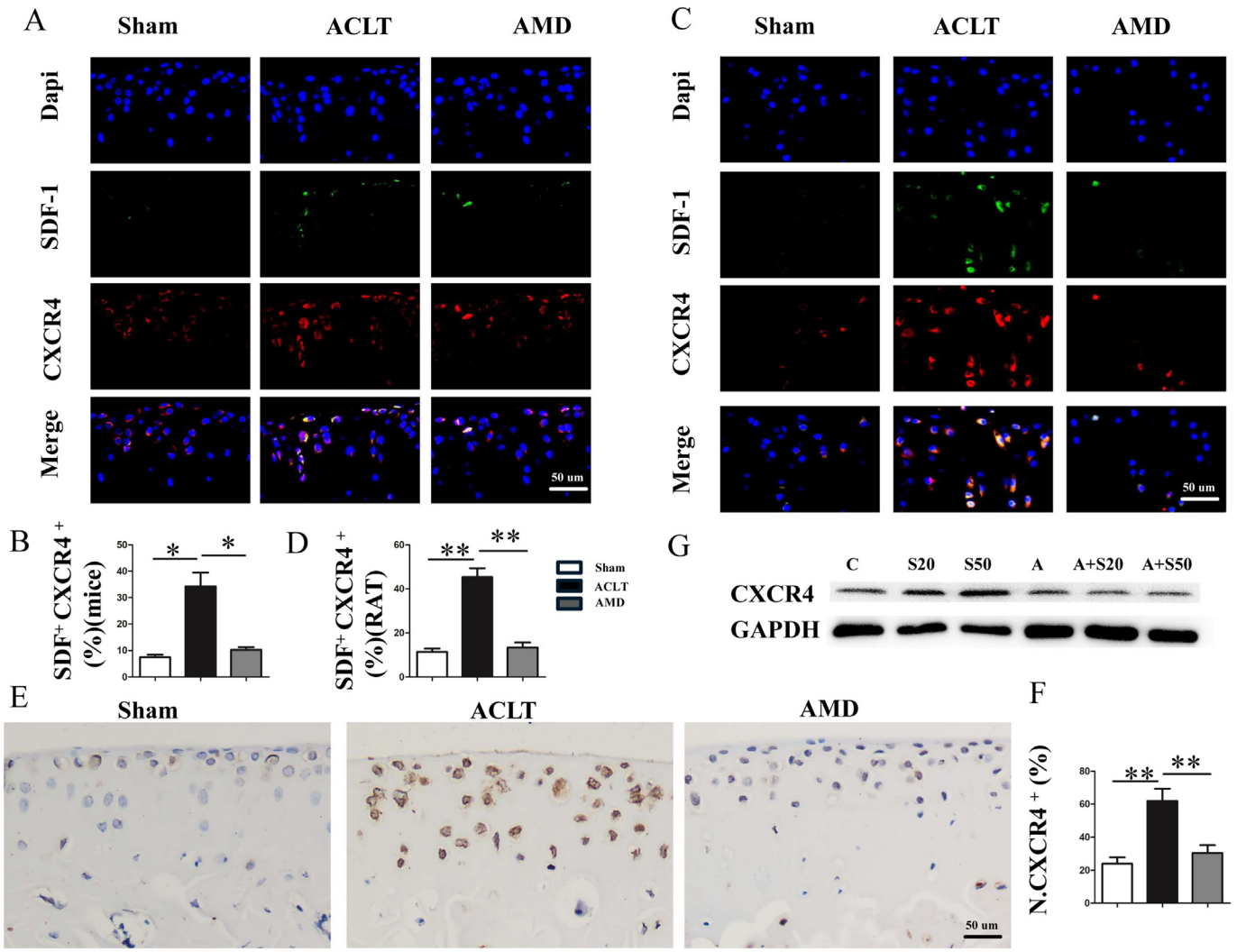

Fig. 4. SDF-1 traverses from the bone to cartilage to link subchondral bone deterioration with articular cartilage degeneration. (A, B) Double-immunofluorescent staining and quantification of SDF and CXCR4 in articular cartilage of mice. $n = 5$. Scale bars, 50 μm. (C, D) Double-immunofluorescent staining and quantitative analysis of SDF and CXCR4 in articular cartilage of rats. n = 5. Scale bars, 50 μm. (E, F) Immunohistochemical staining and quantitative analysis of CXCR4 in articular cartilage of mice. n = 5. Scale bars, 50 μm. (G) Western Blot. The expression of CXCR4 in Chondrocytes after treated with SDF-1 for 24 h with or without 2 hr-pretreatment AMD3100. Sham = sham-surgery; ACLT = ACLT-surgery treated with vehicle; AMD3100 = ACLT-surgery treated with AMD3100. C = control, S20 = SDF-1 (20 ng/ml), S50 = SDF-1 (50 ng/ml), A = AMD3100 (200 ng/ml), A + S20 = AMD3100 (200 ng/ml) + SDF-1(20 ng/ml), A + S50 = AMD3100 (200 ng/ml) + SDF-1 (50 ng/ml). $^{*}p < 0.05$, $^{**}p < 0.01$ compared as denoted by bar.

synovium may accelerate but not trigger cartilage destruction during OA progression. We here demonstrated that tibial subchondral bone deterioration occurred since 14 d after surgery, while alteration in synovium and cartilage began 30 d after surgery, following subchondral bone deterioration. So, infiltration of SDF-1 from synovium is attributed to the damaged integrity of cartilage structure caused by subchondral bone deterioration. Thus, SDF-1 in synovium may have no chance to infiltrate into chondrocytes in vivo if we maintain the homeostasis and integrity of overlying cartilage by normalizing of subchondral bone microarchitecture. Indeed, we revealed that stabilization of subchondral bone structure using AMD3100, administrated by osmotic infusion pumps in subchondral bone specifically significantly lowered SDF-1 in articular cartilage in comparison with vehicle-treated ACLT rodent model, protecting the integrity of overlying cartilage.

SDF-1/CXCR4 axis leads to subchondral bone deterioration by inducing erroneous recruitment of MSCs and excessive bone resorption in subchondral bone. It has been previously reported that increased bone remodeling in subchondral bone is a key point in OA pathogenesis [9,16]. After ACLT, abnormal mechanical loading induces excessive bone resorption in subchondral bone, which liberates excessive cytokines and molecules embedded in the bone matrix leading to erroneous recruitment of MSCs to bone marrow but not to bone resorption sites [16]. We here also found increased bone remodeling in subchondral bone, as demonstrated by elevated Trap and Nestin positive cells. Although the identity of MSCs is still not straightforward, however, in adult bone marrow, Nestin+ cells have been shown to represent a subset of bone marrow precursor cells mainly in endothelial cell lineage and mesenchymal lineage [46]. And Nestin+ cells and leptin receptor-positive (LepR+) cells are major osteoblast-forming mesenchymal stromal precursor cells (MSPCs) in adult bone marrow [47,48]. SDF-1 is a well-known factor that regulates the migration and osteogenic differentiation of MSCs [45]. Previous studies have shown that inhibition of SDF-1/CXCR4 signaling can ameliorate OA development [36,49,50]. However, they did not explore the impact of SDF-1/CXCR4 axis on the crosstalk between subchondral bone and articular cartilage during OA pathogenesis and their inhibitor of SDF-1/CXCR4 signaling was administrated systemically. In this study, we revealed that SDF-1/CXCR4 axis indeed played a vital role in increased bone remodeling of subchondral bone during OA pathogenesis. pErk, the downstream signaling of SDF-1, was elevated significantly during early

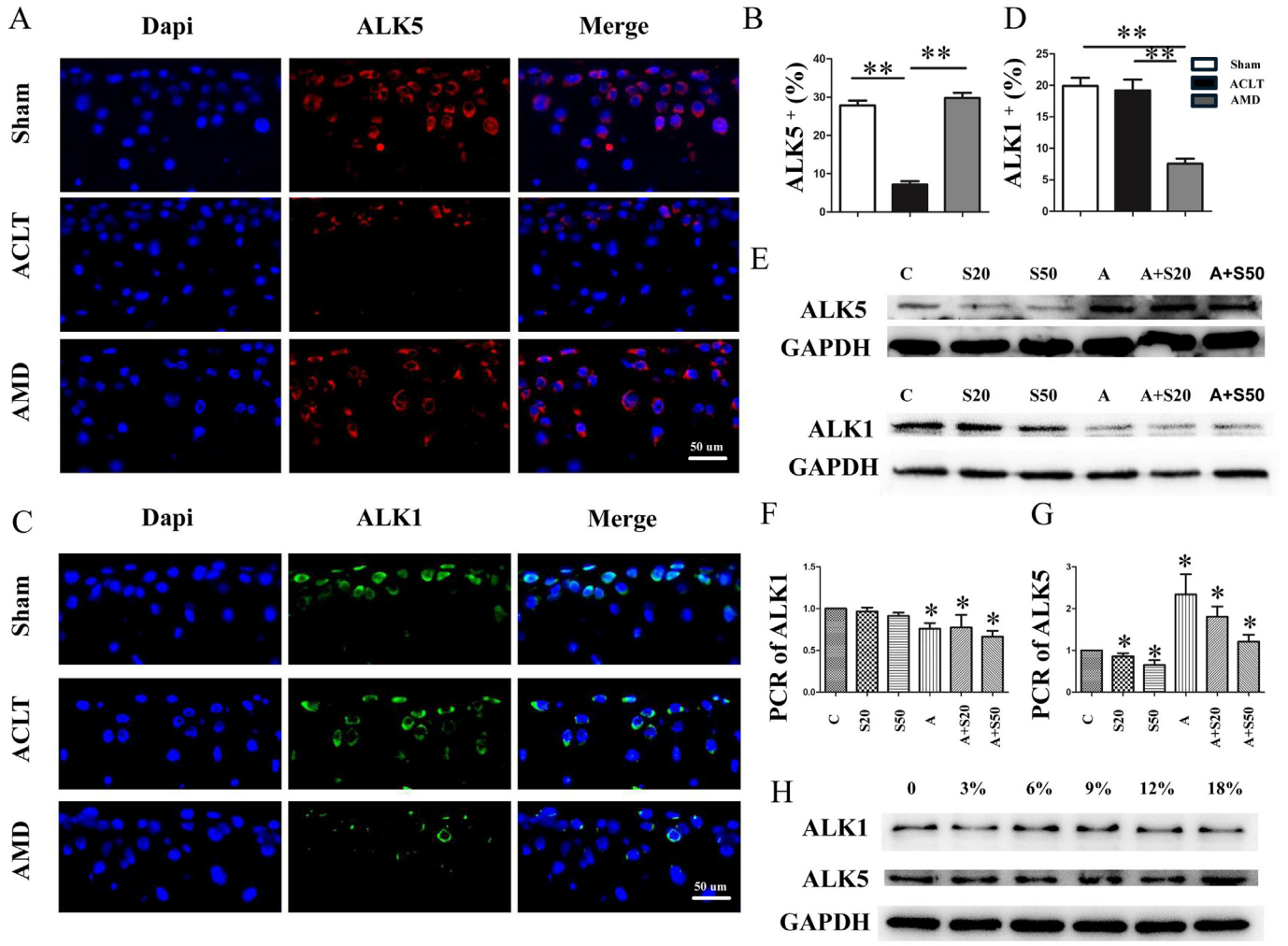

Fig. 5. The shift of TβRI expression in chondrocytes from ALK5 to ALK1 in ACLT mice. (A–D) Immunofluorescent staining and quantitative analysis of ALK5, ALK1 in articular cartilage from mice at 30 days after surgery. $n = 5$. Scale bars, 50 μm. (E–G) Western-blot analysis (E) and RT-PCR (F,G) of ALK5, ALK1 in Chondrocytes after treated with SDF-1 for 24 h with or without 2 h-pretreatment AMD3100. (H) Western Blot. Expression of ALK5 and ALK1 in cartilage on different mechanical stress. Sham = sham-surgery. ACLT = ACLT-surgery treated with vehicle. AMD = ACLT-surgery treated with AMD3100. C = control, S20 = SDF-1 (20 ng/ml), S50 = SDF-1 (50 ng/ml), A = AMD3100 (200 ng/ml), A + S20 = AMD3100 (200 ng/ml) + SDF-1 (20 ng/ml), A + S50 = AMD3100 (200 ng/ml) + SDF-1 (50 ng/ml). $^{*}p < 0.05$, $^{**}p < 0.01$ compared as denoted by bar.

stage of OA. Of note, specific inhibition of SDF-1/CXCR4 axis using AMD3100 via osmotic infusion pumps suppressed phosphorylation of Erk, then normalized the expression of Nestin, LepR and Osterix in subchondral bone. Further, we also demonstrated that targeted inhibition of the SDF-1/CXCR4 axis suppressed bone resorption of subchondral bone, as defined by reduced MMP9-positive osteoclastic cells in subchondral bone relative to vehicle-treated ACLT rats. Excessive bone resorption has a capacity of indirect induction of erroneous MSCs recruitment by excessive liberation of cytokines and molecules embedded in bone marrow matrix [16]. Thus taken together, SDF-1/CXCR4 axis plays a pivotal role in subchondral bone deterioration by inducing erroneous MSCs recruitment directly and indirectly.

SDF-1 traverses from the bone to cartilage to couple subchondral bone deterioration with articular cartilage degeneration. It is known that the interface between the subchondral bone and calcified layer of cartilage lies subchondral bone plate (SBP). In a normal situation, SBP acts as impenetrable barriers to sustain the homeostasis and integrity of overlying cartilage. However, during the onset of OA, SBP porosity increases, allowing larger molecules to traverse the subchondral plate to link subchondral bone deterioration and articular cartilage degeneration [28,29]. The present study found that SDF-1 elevated significantly in the articular cartilage in vehicle-treated ACLT rodent model and that normalization of subchondral bone microarchitecture by specific administration of AMD3100 in subchondral bone returned SDF-1 in cartilage back to its normal level comparable with sham controls. These imply that elevation of SDF-1 in cartilage may be associated with underlying subchondral bone. It is known that subchondral bone during OA development undergoes uncoupled bone remodeling [16], which might lead to enlargement of SBP porosity to allow SDF-1 to traverse from subchondral bone to overlying cartilage. The bone resorption and bone formation during uncoupled bone remodeling do not coordinate well or do not occur at specific anatomical sites, resulting in bone formation not in the bone resorption area, thus formation of osteoid islets and enlargement of subchondral plate porosity.

The present study also demonstrated that SDF-1/CXCR4 axis induced articular cartilage degradation by promoting the shift of TβRI expression in chondrocytes from ALK5 to ALK1. Previous research has shown that CXCR4 is primarily expressed by the articular chondrocytes [35] and SDF-1 is its only known ligand [51]. And It has been well investigated that the maintenance of articular cartilage metabolic homeostasis and structural integrity relies on TGF-β and its downstream signaling [52]. The balance between signaling via either ALK5 or ALK1 is able to determine the response of chondrocytes to TGF-β stimulation,

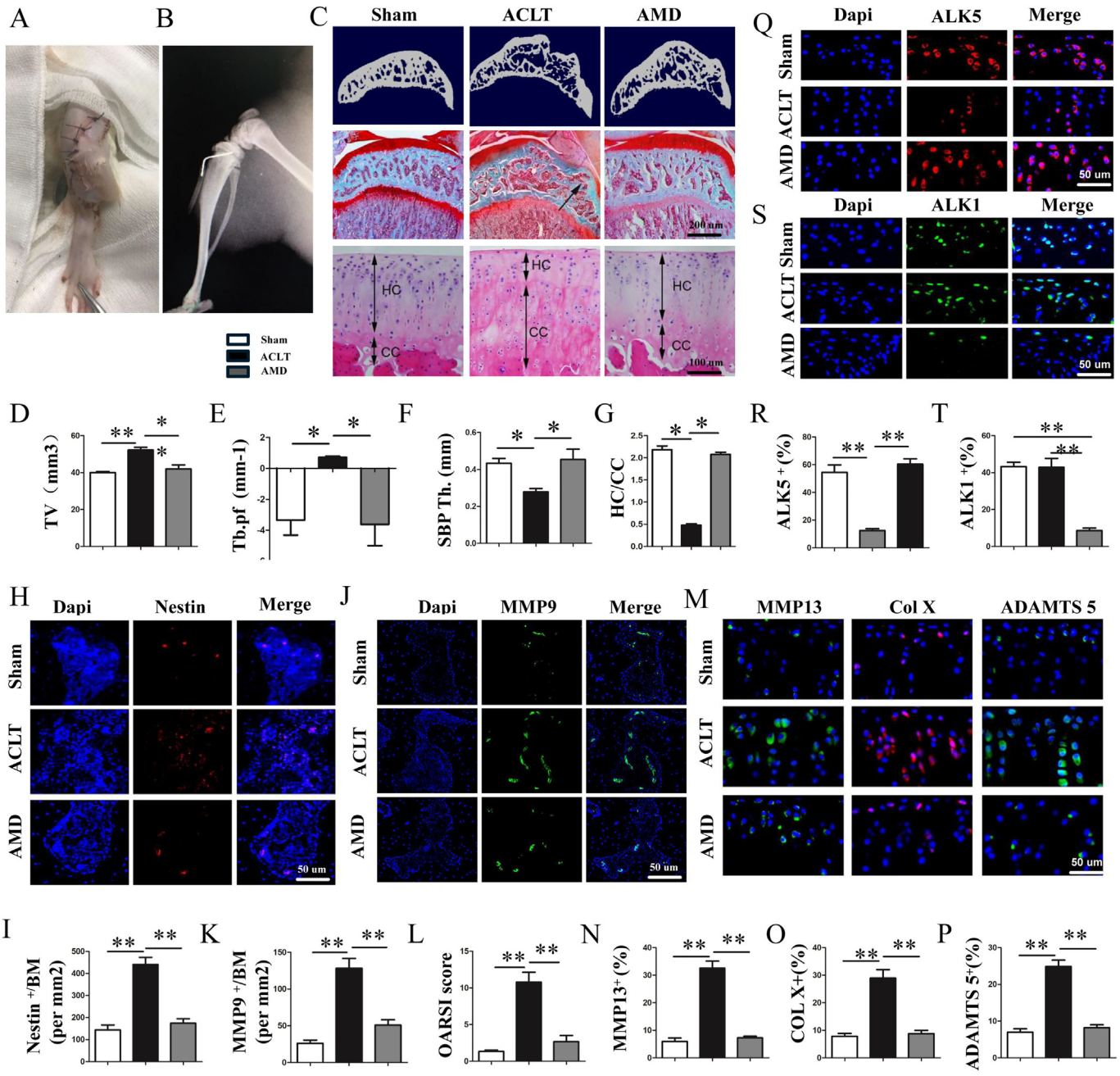

Fig. 6. Specific inhibition of SDF-1/CXCR4 axis in subchondral bone in rats. (A, B) Osmotic infusion pump implanted directly in subchondral bone of rats. (C) Representative three dimensional micro-CT images of sagittal views of subchondral bone medial compartment (TOP); Safranin O and fast green staining (middle) with solid arrows indicating proteoglycan loss and cartilage destruction (Scale bar, 100 μm), H&E staining (bottom) where double-headed arrows to marker calcified cartilage (CC) and hyaline cartilage (HC) thickness (Scale bars, 50 μm). (D–G) Quantitative micro-CT analysis of tibial subchondral bone of total tissue volume (TV) (D), trabecular pattern factor (Tb.pf) (E), subchondral bone plate thickness (F) and HC/CC ratio in cartilage (G). $n = 5$ per group. (H–K) Immunofluorescent staining and quantitative analysis of Nestin$^+$, MMP9$^+$ cells. $n = 5$. Scale bars, 50 μm. (L) Osteoarthritis Research Society International–modified Mankin scores of articular cartilage at 60 days after surgery. n = 5. (M-P) Immunofluorescent staining and quantitative analysis of MMP13, Col X and ADAMTS5 in articular cartilage. n = 5 per group. Scale bars, 50 μm. (Q–T) Immunofluorescent staining and quantitative analysis of ALK1, ALK5 in articular cartilage. n = 5 per group. Scale bars, 50 μm. Sham = sham-surgery. ACLT = ACLT-surgery treated with vehicle. AMD3100 = ACLT-surgery treated with AMD3100. *$p < 0.05$ **$p < 0.01$ compared as denoted by bar.

which is anabolic through ALK5 induced Smad2/3 signaling while catabolic through ALK1 induced Smad1/5/8 pathway [23–25]. We found that SDF-1/CXCR4 axis in chondrocytes resulted in the shift of TβRI expression in chondrocytes from a dominant ALK5 to a more pronounced ALK1, with the ratio of ALK1/ALK5 increased. Of note, inhibition of SDF-1/CXCR4 axis, both systemic and specific administration of AMD3100 in subchondral bone, normalized the ALK1/ALK5 ratio in articular cartilage and ameliorated the onset of OA. The impact of specific administration of AMD300 in subchondral bone on the balance between ALK1 and ALK5 in cartilage might be attributed to normalization of subchondral bone microarchitecture by specific inhibition of SDF-1/CXCR4 axis in subchondral bone. This might results in the inability of SDF-1 to traverse SBP to combine with CXCR4 in the articular chondrocytes.

CXCR7, previously named RDC1, has been recently identified as a novel receptor for SDF-1 [53]. Unlike CXCR4, CXCR7 activation does

not promote cell migration. Rather, CXCR7 induces cell growth, angiogenesis and protection from apoptosis [33]. It has also been reported that CXCR7 is expressed in cartilage and synovial fibroblasts, which has evoked great attention towards the investigation of the role of CXCR7 on rheumatoid arthritis [54,55]. Additionally, recent papers reveal that CXCR7 participates in the modulation of CXCR4 signaling, because it is able to heterodimerize with CXCR4 [56,57]. Thus, CXCR7 might also be a promising target towards OA pathogenesis.

This study found that SDF-1/CXCR4 axis might promote OA progression by coupling subchondral bone deterioration and articular cartilage degeneration. Specific inhibition of SDF-1/CXCR4 axis in subchondral bone using osmotic infusion pumps stabilized subchondral bone microarchitecture by normalization of erroneous MSCs recruitment and abnormal bone resorption, and then ameliorated articular cartilage degradation by abrogation of the shift of TβRI expression in chondrocytes from ALK5 to ALK1. Taken together, our findings may provide a mechanistic insight into how SDF-1/CXCR4 axis regulates the crosstalk between subchondral bone and articular cartilage in OA pathogenesis.

Declaration of Competing Interest

The author(s) declare that they have no competing interests.

Acknowledgments

This study was supported by National Natural Science Foundation of China (81601942 to ZC; 81600013 to TX; 81830079 to BY); Outstanding Youths Development Scheme of Nanfang Hospital, Southern Medical University (2017J011 to ZC) and President Foundation of Nanfang Hospital, Southern Medical University (2015C011 to ZC).

Appendix A. Supplementary data

Supplementary data to this article can be found online at https://doi.org/10.1016/j.bone.2019.05.010.

References

[1] D.T. Felson, Clinical practice. Osteoarthritis of the knee, N. Engl. J. Med. 354 (8) (2006) 841–848.
[2] D. Blalock, A. Miller, M. Tilley, J. Wang, Joint instability and osteoarthritis, Clin. Med. Insights Arthritis Musculoskelet. Disord. 8 (2015) 15–23.
[3] R.C. Lawrence, D.T. Felson, C.G. Helmick, L.M. Arnold, H. Choi, R.A. Deyo, et al., Estimates of the prevalence of arthritis and other rheumatic conditions in the United States. Part II, Arthritis Rheum. 58 (1) (2008) 26–35.
[4] F. Berenbaum, Osteoarthritis year 2010 in review: pharmacological therapies, Osteoarthr. Cartil. 19 (4) (2011) 361–365.
[5] G.A. Hawker, S. Mian, K. Bednis, Osteoarthritis year 2010 in review: non-pharmacologic therapy, Osteoarthr. Cartil. 19 (4) (2011) 366–374.
[6] D.M. Findlay, J.S. Kuliwaba, Bone-cartilage crosstalk: a conversation for understanding osteoarthritis, Bone Res. 4 (2016) 16028.
[7] Y. Chen, Y. Hu, Y.E. Yu, X. Zhang, T. Watts, B. Zhou, et al., Subchondral trabecular rod loss and plate thickening in the development of osteoarthritis, J. Bone Miner. Res. 33 (2) (2018) 316–327.
[8] G.H. Lo, M.G. Merchant, J.B. Driban, J. Duryea, L.L. Price, C.B. Eaton, et al., Knee alignment is quantitatively related to periarticular bone morphometry and density, especially in patients with osteoarthritis, Arthritis Rheumatol. 70 (2) (2018) 212–221.
[9] D.B. Burr, M.A. Gallant, Bone remodelling in osteoarthritis, Nat. Rev. Rheumatol. 8 (11) (2012) 665–673.
[10] R.J. Lories, F.P. Luyten, The bone-cartilage unit in osteoarthritis, Nat. Rev. Rheumatol. 7 (1) (2011) 43–49.
[11] J. Pan, B. Wang, W. Li, X. Zhou, T. Scherr, Y. Yang, et al., Elevated cross-talk between subchondral bone and cartilage in osteoarthritic joints, Bone 51 (2) (2012) 212–217.
[12] J.C. Baker-LePain, N.E. Lane, Role of bone architecture and anatomy in osteoarthritis, Bone 51 (2) (2012) 197–203.
[13] F.W. Roemer, A. Guermazi, M.K. Javaid, J.A. Lynch, J. Niu, Y. Zhang, et al., Change in MRI-detected subchondral bone marrow lesions is associated with cartilage loss: the MOST Study. A longitudinal multicentre study of knee osteoarthritis, Ann. Rheum. Dis. 68 (9) (2009) 1461–1465.
[14] J.P. Raynauld, J. Martel-Pelletier, M.J. Berthiaume, F. Abram, D. Choquette, B. Haraoui, et al., Correlation between bone lesion changes and cartilage volume loss in patients with osteoarthritis of the knee as assessed by quantitative magnetic resonance imaging over a 24-month period, Ann. Rheum. Dis. 67 (5) (2008) 683–688.
[15] S. Zhu, K. Chen, Y. Lan, N. Zhang, R. Jiang, J. Hu, Alendronate protects against articular cartilage erosion by inhibiting subchondral bone loss in ovariectomized rats, Bone 53 (2) (2013) 340–349.
[16] G. Zhen, C. Wen, X. Jia, Y. Li, J.L. Crane, S.C. Mears, et al., Inhibition of TGF-β signaling in mesenchymal stem cell of subchondral bone attenuates osteoarthritis, Nat. Med. 19 (6) (2013) 704–712.
[17] Z. Cui, J. Crane, H. Xie, X. Jin, G. Zhen, C. Li, et al., Halofuginone attenuates osteoarthritis by inhibition of TGF-β activity and H-type vessel formation in subchondral bone, Ann. Rheum. Dis. 75 (9) (2016) 1714–1721.
[18] Z. Cui, C. Xu, X. Li, J. Song, B. Yu, Treatment with recombinant lubricin attenuates osteoarthritis by positive feedback loop between articular cartilage and subchondral bone in ovariectomized rats, Bone 74 (2015) 37–47.
[19] J. Shen, S. Li, D. Chen, TGF-β signaling and the development of osteoarthritis, Bone Res. 2 (2014) (pii:14002).
[20] P.M. van der Kraan, M.J. Goumans, E. Blaney Davidson, P. ten Dijke, Age-dependent alteration of TGF-β signalling in osteoarthritis, Cell Tissue Res. 347 (1) (2012) 257–265.
[21] E.N. Blaney Davidson, D.F. Remst, E.L. Vitters, H.M. van Beuningen, A.B. Blom, M.J. Goumans, et al., Increase in ALK1/ALK5 ratio as a cause for elevated MMP-13 expression in osteoarthritis in humans and mice, J. Immunol. 182 (12) (2009) 7937–7945.
[22] C.H. Heldin, K. Miyazono, P. ten Dijke, TGF-beta signalling from cell membrane to nucleus through SMAD proteins, Nature 390 (6659) (1997) 465–471.
[23] P.M. van der Kraan, E.N. Blaney Davidson, W.B. van den Berg, A role for age-related changes in TGFbeta signaling in aberrant chondrocyte differentiation and osteoarthritis, Arthritis Res. Ther. 12 (1) (2010) 201.
[24] M.J. Goumans, G. Valdimarsdottir, S. Itoh, F. Lebrin, J. Larsson, C. Mummery, et al., Activin receptor-like kinase (ALK)1 is an antagonistic mediator of lateral TGFbeta/ALK5 signaling, Mol. Cell 12 (4) (2003) 817–828.
[25] K.W. Finnson, W.L. Parker, P. ten Dijke, M. Thorikay, A. Philip, ALK1 opposes ALK5/Smad3 signaling and expression of extracellular matrix components in human chondrocytes, J. Bone Miner. Res. 23 (6) (2008) 896–906.
[26] J.M. Clark, J.D. Huber, The structure of the human subchondral plate, J. Bone Joint Surg. Br. 72 (5) (1990) 866–873.
[27] H. Duncan, J. Jundt, J.M. Riddle, W. Pitchford, T. Christopherson, The tibial subchondral plate. A scanning electron microscopic study, J. Bone Joint Surg. Am. 69 (8) (1987) 1212–1220.
[28] S.M. Botter, G.J. van Osch, S. Clockaerts, J.H. Waarsing, H. Weinans, J.P. van Leeuwen, Osteoarthritis induction leads to early and temporal subchondral plate porosity in the tibial plateau of mice: an in vivo microfocal computed tomography study, Arthritis Rheum. 63 (9) (2011) 2690–2699.
[29] H. Iijima, T. Aoyama, J. Tajino, A. Ito, M. Nagai, S. Yamaguchi, et al., Subchondral plate porosity colocalizes with the point of mechanical load during ambulation in a rat knee model of post-traumatic osteoarthritis, Osteoarthr. Cartil. 24 (2) (2016) 354–363.
[30] A. Kortesidis, A. Zannettino, S. Isenmann, S. Shi, T. Lapidot, S. Gronthos, Stromal-derived factor-1 promotes the growth, survival, and development of human bone marrow stromal stem cells, Blood 105 (10) (2005) 3793–3801.
[31] G. Lisignoli, S. Toneguzzi, A. Piacentini, S. Cristino, F. Grassi, C. Cavallo, et al., CXCL12 (SDF-1) and CXCL13 (BCA-1) chemokines significantly induce proliferation and collagen type I expression in osteoblasts from osteoarthritis patients, J. Cell. Physiol. 206 (1) (2006) 78–85.
[32] K. Kanbe, K. Takagishi, Q. Chen, Stimulation of matrix metalloprotease 3 release from human chondrocytes by the interaction of stromal cell-derived factor 1 and CXC chemokine receptor 4, Arthritis Rheum. 46 (1) (2002) 130–137.
[33] A. Villalvilla, R. Gomez, J.A. Roman-Blas, R. Largo, G. Herrero-Beaumont, SDF-1 signaling: a promising target in rheumatic diseases, Expert Opin. Ther. Targets 18 (9) (2014) 1077–1087.
[34] K. Kanbe, T. Takemura, K. Takeuchi, Q. Chen, K. Takagishi, K. Inoue, Synovectomy reduces stromal-cell-derived factor-1 (SDF-1) which is involved in the destruction of cartilage in osteoarthritis and rheumatoid arthritis, J. Bone Joint Surg. Br. 86 (2) (2004) 296–300.
[35] K. Kanbe, K. Takagishi, Q. Chen, Stimulation of matrix metalloprotease 3 release from human chondrocytes by the interaction of stromal cell-derived factor 1 and CXC chemokine receptor 4, Arthritis Rheum. 46 (1) (2002) 130–137.
[36] Y. Chen, S. Lin, Y. Sun, J. Guo, Y. Lu, C.W. Suen, et al., Attenuation of subchondral bone abnormal changes in osteoarthritis by inhibition of SDF-1 signaling, Osteoarthr. Cartil. 25 (6) (2017) 986–994.
[37] R. Mohle, F. Bautz, S. Rafii, M.A. Moore, W. Brugger, L. Kanz, The chemokine receptor CXCR-4 is expressed on CD34+ hematopoietic progenitors and leukemic cells and mediates transendothelial migration induced by stromal cell-derived factor-I, Blood 91 (12) (1998) 4523–4530.
[38] R. Datema, L. Rabin, M. Hincenbergs, M.B. Moreno, S. Warren, V. Linquist, et al., Antiviral efficacy in vivo of the anti-human immunodeficiency virus bicyclam SDZ SID 791 (JM3100), an inhibitor of infectious cell entry, Antimicrob. Agents Chemother. 40 (3) (1996) 750–754.
[39] P. Matthys, S. Hatse, K. Vermeire, A. Wuyts, G. Bridger, G.W. Henson, et al., AMD3100, a potent and specific antagonist of the stromal cell-derived factor-1 chemokine receptor CXCR4, inhibits autoimmune joint inflammation in IFN-gamma receptor-deficient mice, J. Immunol. 167 (8) (2001) 4686–4692.
[40] A. Patel, T. Mehta, J. Patel, M. Patel, K. Patel, N. Patel, Recent advances in

asymmetric membrane capsule based osmotic pump: a patent overview, Recent Pat. Drug Deliv. Formul. 6 (1) (2012) 66–72.
[41] K.P. Pritzker, S. Gay, S.A. Jimenez, K. Ostergaard, J.P. Pelletier, P.A. Revell, et al., Osteoarthritis cartilage histopathology: grading and staging, Osteoarthr. Cartil. 14 (1) (2006) 13–29.
[42] J. Gong, H.B. Meng, J. Hua, Z.S. Song, Z.G. He, B. Zhou, et al., The SDF-1/CXCR4 axis regulates migration of transplanted bone marrow mesenchymal stem cells towards the pancreas in rats with acute pancreatitis, Mol. Med. Rep. 9 (5) (2014) 1575–1582.
[43] Q. Liu, X. Hu, X. Zhang, X. Duan, P. Yang, F. Zhao, et al., Effects of mechanical stress on chondrocyte phenotype and chondrocyte extracellular matrix expression, Sci. Rep. 6 (2016) 37268.
[44] C. Liu, Y. Weng, T. Yuan, H. Zhang, H. Bai, B. Li, et al., CXCL12/CXCR4 signal axis plays an important role in mediating bone morphogenetic protein 9-induced osteogenic differentiation of mesenchymal stem cells, Int. J. Med. Sci. 10 (9) (2013) 1181–1192.
[45] N. Hosogane, Z. Huang, B.A. Rawlins, X. Liu, O. Boachie-Adjei, A.L. Boskey, et al., Stromal derived factor-1 regulates bone morphogenetic protein 2-induced osteogenic differentiation of primary mesenchymal stem cells, Int. J. Biochem. Cell Biol. 42 (7) (2010) 1132–1141.
[46] S. Méndez-Ferrer, T.V. Michurina, F. Ferraro, A.R. Mazloom, B.D. Macarthur, S.A. Lira, et al., Mesenchymal and haematopoietic stem cells form a unique bone marrow niche, Nature 466 (7308) (2010) 829–834.
[47] B.O. Zhou, R. Yue, M.M. Murphy, J.G. Peyer, S.J. Morrison, Leptin-receptor-expressing mesenchymal stromal cells represent the main source of bone formed by adult bone marrow, Cell Stem Cell 15 (2) (2014) 154–168.
[48] X. Wang, L. Xie, J. Crane, G. Zhen, F. Li, P. Yang, et al., Aberrant TGF-β activation in bone tendon insertion induces enthesopathy-like disease, J. Clin. Invest. 128 (2) (2018) 846–860.
[49] Y. Dong, H. Liu, X. Zhang, F. Xu, L. Qin, P. Cheng, et al., Inhibition of SDF-1α/CXCR4 signalling in subchondral bone attenuates post-traumatic osteoarthritis, Int. J. Mol. Sci. 17 (6) (2016) (pii:E943).
[50] F. Wei, D.C. Moore, L. Wei, Y. Li, G. Zhang, X. Wei, et al., Attenuation of osteoarthritis via blockade of the SDF-1/CXCR4 signaling pathway, Arthritis Res. Ther. 14 (4) (2012) R177.
[51] K.E. McGrath, A.D. Koniski, K.M. Maltby, J.K. McGann, J. Palis, Embryonic expression and function of the chemokine SDF-1 and its receptor, CXCR4, Dev. Biol. 213 (2) (1999) 442–456.
[52] X. Yang, L. Chen, X. Xu, C. Li, C. Huang, C.X. Deng, TGF-beta/Smad3 signals repress chondrocyte hypertrophic differentiation and are required for maintaining articular cartilage, J. Cell Biol. 153 (1) (2001) 35–46.
[53] J.M. Burns, B.C. Summers, Y. Wang, A. Melikian, R. Berahovich, Z. Miao, et al., A novel chemokine receptor for SDF-1 and I-TAC involved in cell survival, cell adhesion, and tumor development, J. Exp. Med. 203 (2006) 2201–2213.
[54] L. Wei, K. Kanbe, M. Lee, X. Wei, M. Pei, X. Sun, et al., Stimulation of chondrocyte hypertrophy by chemokine stromal cell-derived factor 1 in the chondro-osseous junction during endochondral bone formation, Dev. Biol. 341 (1) (2010) 236–245.
[55] K. Watanabe, M.E. Penfold, A. Matsuda, N. Ohyanagi, K. Kaneko, Y. Miyabe, et al., Pathogenic role of CXCR7 in rheumatoid arthritis, Arthritis Rheum. 62 (11) (2010) 3211–3220.
[56] F.M. Décaillot, M.A. Kazmi, Y. Lin, S. Ray-Saha, T.P. Sakmar, P. Sachdev, CXCR7/CXCR4 heterodimer constitutively recruits beta-arrestin to enhance cell migration, J. Biol. Chem. 286 (37) (2011) 32188–32197.
[57] A. Levoye, K. Balabanian, F. Baleux, F. Bachelerie, B. Lagane, CXCR7 heterodimerizes with CXCR4 and regulates CXCL12-mediated G protein signaling, Blood 113 (24) (2009) 6085–6093.